Novel 4DCT Method to Measure Regional Left Ventricular Endocardial Shortening Before and After Transcatheter Mitral Valve Implantation

Gabrielle M. Colvert, Ashish Manohar, Francisco J. Contijoch, James Yang, Jeremy Glynn, Philipp Blanke, Jonathon A. Leipsic & Elliot R. McVeigh

Published online: 15 Jul 2021.

Submit your article to this journal

Article views: 24

View related articles

View Crossmark data

ORIGINAL RESEARCH

Novel 4DCT Method to Measure Regional Left Ventricular Endocardial Shortening Before and After Transcatheter Mitral Valve Implantation

Gabrielle M. Colvert, PhD [a], Ashish Manohar, PhD[b], Francisco J. Contijoch, PhD[a,c], James Yang, BS[d], Jeremy Glynn, PhD[e], Philipp Blanke, MD[f], Jonathon A. Leipsic, MD[f], and Elliot R. McVeigh, PhD[a,c,g]

aDepartment of Bioengineering, University of California San Diego, La Jolla, California, USA; bDepartment of Mechanical and Aerospace Engineering, University of California San Diego, La Jolla, California, USA; cDepartment of Radiology, University of California San Diego, La Jolla, California, USA; dDepartment of Biological Sciences, University of California San Diego, La Jolla, California, USA; eAbbott Medical, St. Paul, Minnesota, USA; fSt. Paul's Hospital, University of British Columbia, Vancouver, British Columbia, Canada; gDepartment of Medicine, Cardiovascular Division, University of California San Diego, La Jolla, California, USA

ABSTRACT

Background: Regional left ventricular (LV) mechanics in mitral regurgitation (MR) patients, and local changes in function after transcatheter mitral valve implantation (TMVI) have yet to be evaluated. Herein, we introduce a method for creating high resolution maps of endocardial function from 4DCT images, leading to detailed characterization of changes in local LV function. These changes are particularly interesting when evaluating the effect of the TendyneTM TMVI device in the region of the epicardial pad.

Methods: Regional endocardial shortening from CT (RS_{CT}) was evaluated in Tendyne (Abbott Medical) TMVI patients with 4DCT exams pre- and post-implantation. Regional function was evaluated in 90 LV segments (5 longitudinal x 18 circumferential). LV volumes and ejection fraction (EF) were also computed. A reproducibility study was performed in a subset of patients to determine the precision of RS_{CT} measurements in this population.

Results: Baseline and local changes in RS_{CT} post TMVI were highly variable and extremely spatially heterogeneous. Both inter- and intra-observer variability were low and demonstrated the high precision of RS_{CT} for evaluating regional LV function.

Conclusion: RS_{CT} is a reproducible metric which can be evaluated in patients with highly abnormal regional LV function and geometry. After TMVI, significant spatially heterogeneous changes in RS_{CT} were observed in all subjects; therefore, it is unlikely that the functional state of TMVI patients can be fully described by changes in LV volume or EF. Measurement of RS_{CT} provides precise characterization of the spatially heterogeneous effects of MR and TMVI on LV function and remodeling.

Abbreviations: LV: Left Ventricle; MR: Mitral Regurgitation; TMVI: Transcatheter Mitral Valve Implantation; EP: Epicardial Pad; RS_{CT}: CT Regional Endocardial Shortening; ED: End Diastole; ES: End Systole; EF: Ejection Fraction; LVOT: Left Ventricular Outflow Tract

Introduction

In addition to improvements in bioprosthetic devices and surgical technologies, advances in noninvasive imaging have supported the outcomes of transcather procedures.[1,2] Their role has expanded from anatomical pre-procedural planning to include analysis of cardiac physiology for diagnosis, peri-procedural guidance, and post-procedural follow-up.[1,3,4] Therefore, noninvasive imaging also has the potential to help determine which patients will benefit from valve repair or replacement procedures based on quantifiable prognostic parameters.[4–6]

Typically, left ventricular (LV) ejection fraction (EF) is a parameter used to quantify cardiac function as well as eligibility and fitness for certain procedures. According to the AHA/ACC guidelines for valvular heart disease, surgery is a Class I indication for patients with severe primary MR and LVEF >30%; in contrast there is only a Class IIb

indication for surgery in those with LVEF <30%.[7] However, when mitral regurgitation (MR) is present, EF may not adequately represent LV systolic function because a significant proportion of the stroke volume flows retrograde into the left atrium,[8] and it has been shown that EF is a late indicator of LV dysfunction.[9,10] As an alternative, recent studies have demonstrated that myocardial deformation parameters, such as global longitudinal and circumferential strain, are more sensitive measures and can be utilized to detect disease earlier than significant changes in EF.[11,12] Yet, many patients with secondary MR tend to also have dyssynchronous function and highly regional abnormalities; hence, these global metrics cannot accurately capture the full picture of LV function.[12] High resolution regional measurements of myocardial function could provide a better characterization of the extent of LV dysfunction in patients with MR.

Transcatheter mitral valve implantation (TMVI) is a relatively new procedure for treating MR; however, its effect on regional LV function has yet to be characterized. 4D x-ray computed tomography (4DCT) is a promising method for evaluating changes in regional cardiac function in patients with abnormal LV geometry and local dysfunction because of its high 3D spatial resolution and full heart volume coverage within a single heartbeat.[5,13] The goal of this research was to investigate the feasibility and reproducibility of evaluating 4DCT-derived regional endocardial shortening (RS_{CT}) in patients receiving TMVI. Local areas of hypokinesis and LV dysfunction are frequent in this population and therefore represent a particularly relevant cohort to study regional LV function. RS_{CT} was previously shown to correlate well with MRI-tagging derived myocardial strain and therefore serves as a surrogate of strain in this work.[14] Due to the small cohort of patients, we did not attempt to evaluate factors that correlated with patient outcomes. To the best of our knowledge, this is the first study to use 4DCT to quantify 3D regional LV function in subjects before and after TMVI.

Materials and methods

Subjects

All subjects included in the present analysis were enrolled in the Expanded Clinical Study of the Tendyne Mitral Valve System (NCT02321514) between November 2014 and November 2017 across 24 hospitals. Institutional Review Board approval and informed patient consent was obtained at each of the individual sites. Twenty-four patients treated with TMVI due to significant MR (grade 3 or 4) and deemed unsuitable for conventional mitral valve surgery were considered for analysis. Seven patients were excluded due to the reasons listed in Table 1. In total, 17 subjects had 4DCT exams before and 1-month after TMVI with at least end-diastolic (ED) and end-systolic (ES) phases and were therefore included in this preliminary proof-of-concept study.

The CT exams were conducted at eight different study sites as part of Tendyne's Global feasibility study as previously described.[15] While all 17 subjects were included in the analysis of regional function, 10 subjects had retrospective imaging with full R-R cycles which were analyzable at baseline and 1-month, and 7 subjects had at least ED and ES included in the phases imaged. The subjects were scanned on a single-beat Toshiba Aquilion ONE, multi-beat Siemens SOMATOM Definition, multi-beat Siemens SOMATOM Force, or a multi-beat Philips iCT 256. The minimum and maximum pixel

spacing was 0.344 mm and 1.145 mm, respectively. Lastly, the minimum and maximum slice thickness was 0.5 mm and 1.5 mm, respectively. LV volumes were computed from the 4DCT scans by counting the number of voxels identified as blood pool in the LV segmentation from the tip of the endocardial apex to the mitral valve plane. These volumes excluded the papillary muscles and were used to calculate LVEF.

Analysis of 4DCT-derived regional endocardial shortening

The LV blood pool was segmented from the 4DCT images in 3D using a region-growing algorithm in ITK-SNAP (ver. 3.6.2)-[16] in order to extract the endocardial surface for the analysis. The threshold for segmenting the LV blood pool was determined mathematically using Otsu's method on a region-of-interest in a mid-axial slice at ED containing the contrast-enhanced blood pool and the surrounding myocardium.[17] We obtained a surface representation of the endocardium to include the full LV from the endocardial apical tip to the mitral valve plane.[18] In 3D, two planes were defined manually to separate the left atrium and the LV outflow tract (LVOT) from the LV. The mitral valve plane was cut at the mitral annulus using the posterior segment of the D-shaped annulus as a landmark as this region of the annulus is most planar.[19,20] The plane defining the aortic outflow tract was cut tangent to the surface of the LV blood pool and intersected the left and right trigone where the mitral annulus meets the LVOT.[19] This LV blood pool segmentation was repeated in all timeframes available from the 4DCT. Triangular meshes of the endocardial boundary were extracted from the 3D segmentation using *isosurface* in MATLAB and point-cloud registration was performed on these surfaces in order to obtain 3D displacement fields across the cardiac cycle as previously described.[21,22] Figure 1 summarizes the process of obtaining these displacement fields from the 4DCT data. After point-cloud registration, RS_{CT} was defined as

$$RS_{CT} = \sqrt{\frac{Area(t,x)}{Area(ED,x)}} - 1 \qquad (1)$$

where the area is calculated for face, x, at time, t, and the reference timeframe of ED (Figure 2). A negative RS_{CT} value indicates that the endocardial surface in that region is contracting while a positive RS_{CT} value indicates that the surface is stretching.

Characterization of changes in RS_{CT} between baseline and 1-month after TMVI

High resolution maps of RS_{CT} were measured (90 LV segments, 5 longitudinal x 18 circumferential) in order to capture the highly variable changes in geometry and function of these patients with severe MR, frequent LV dyssynchrony, and local myocardial deformation from the epicardial pad. For the 10 subjects with images spanning the entire R-R cycle, peak RS_{CT} was defined as the minimum point on the RS_{CT} vs. time curves for each segment within a window of ±25% of the time of minimum LV volume. For the seven subjects with images over a partial interval of the R-R cycle, peak RS_{CT} was

Table 1. Reason studies were not analyzed for comparison of 4DCT-derived regional endocardial shortening before and 1-month after TMVI.

Reason for images not analyzed	Number of patients excluded
Irregular Heartbeat (Double beat leading to incomplete ejection of blood)	2
Step Artifact	4
Low contrast between LV blood pool and myocardium (poor contrast injection timing)	1
Total	7/24

defined at the time of minimum LV volume because continuous timeframes were not available for analysis. Bullseye plots were constructed to compare peak RS_{CT} in all 90 segments pre and post TMVI. As the specific anchoring system of the Tendyne TMVI device uses a tether and epicardial pad, abnormal local deformation of the LV was expected in the region near the pad. Therefore, the epicardial pad was identified on the CT images and its location was marked on the bullseye plots (Figure 3).

Normal peak RS_{CT} was measured from a cohort of 23 healthy controls and determined to be -0.32 ± 0.06 averaged over the entire LV. The characteristics of the healthy controls are shown in Table 2. Given the natural variation in RS_{CT} in these normal LVs, peak RS_{CT} in the TMVI patients in each segment was characterized as normal ($RS_{CT} \leq -0.3$), "kinetic" ($-0.3 < RS_{CT} \leq -0.2$), hypokinetic ($-0.2 < RS_{CT} \leq -0.1$), akinetic ($-0.1 < RS_{CT} \leq 0$), and dyskinetic ($RS_{CT} > 0$) as shown in Figure 2. The "kinetic" category between normal and hypokinetic was created in order to distinguish between the subjects who begin with somewhat

normal function despite MR ("kinetic") and those with lower function at baseline (hypokinetic). Eighty-nine percent of Tendyne patients have secondary MR with advanced heart failure[15]; therefore, few patients have normal function, and the precision of RS_{CT} estimates[23] supported creating this additional "kinetic" functional category between normal and hypokinetic.

Statistics

All statistical analyses were performed in MATLAB (2018b, MathWorks Inc.). To determine if changes in ED and ES

Table 2. Characteristics of healthy control group.

N	23
Age, years	60 ± 12
Males (%)	12 (53%)
4DCT-derived LVEF	70% ± 5%
4DCT-derived GLS	21% ± 2%

*Global Longitudinal Strain (GLS), Left Ventricular Ejection Fraction (LVEF).
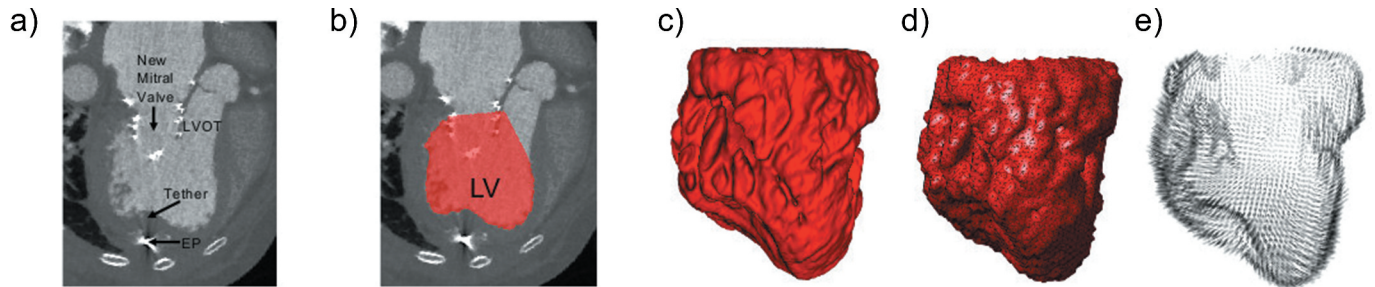

Figure 1. Obtaining 3D endocardial displacement fields from 4DCT data. (a) Contrast-enhanced 4DCT image containing the left ventricle (LV), LV outflow tract (LVOT), and the TMVI device including the tether and epicardial pad (EP), (b) Segmentation of LV blood pool is performed using a region growing algorithm. The threshold for segmentation is determined using Otsu's method, (c) 3D view of segmented LV blood pool, (d) Endocardial surface extracted from the segmentation in MATLAB, E) Point-cloud registration is used to solve for the 3D displacement field of the endocardial surface between timeframes.
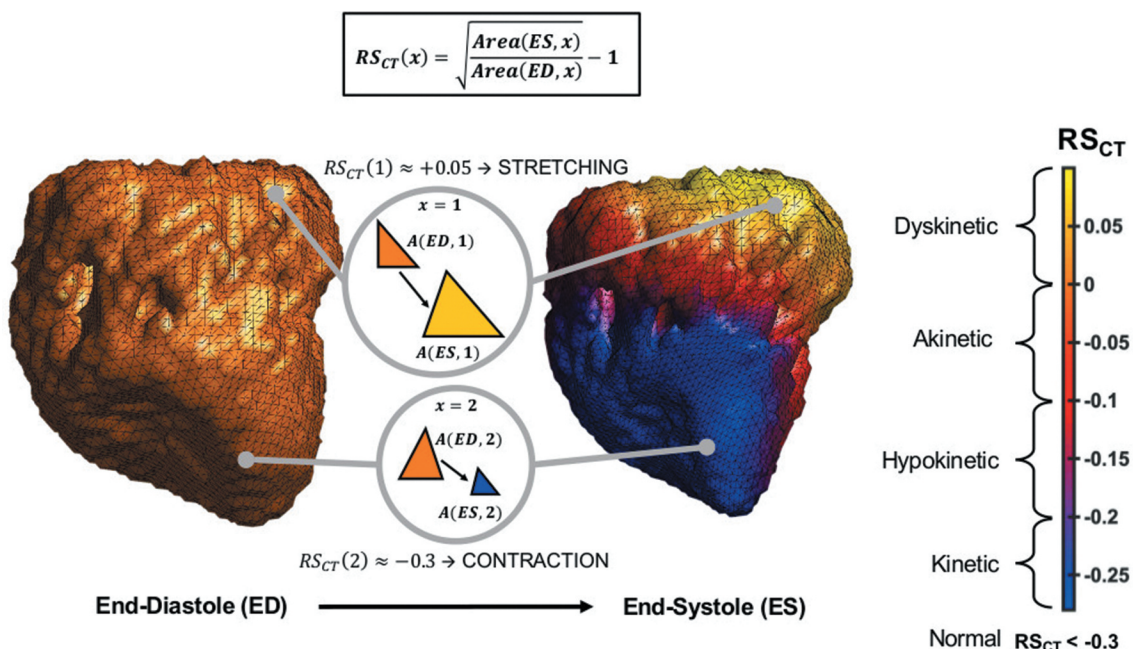
$$RS_{CT}(x) = \sqrt{\frac{Area(ES, x)}{Area(ED, x)}} - 1$$

Figure 2. Measurement and characterization of 4DCT-derived left ventricular endocardial regional shortening (RS_{CT}). RS_{CT} is defined by the equation shown and was characterized as normal ($RS_{CT} \leq -0.3$), kinetic ($-0.3 < RS_{CT} \leq -0.2$), hypokinetic ($-0.2 < RS_{CT} \leq -0.1$), akinetic ($-0.1 < RS_{CT} \leq 0$), and dyskinetic ($RS_{CT} > 0$) before and 1-month after TMVI.
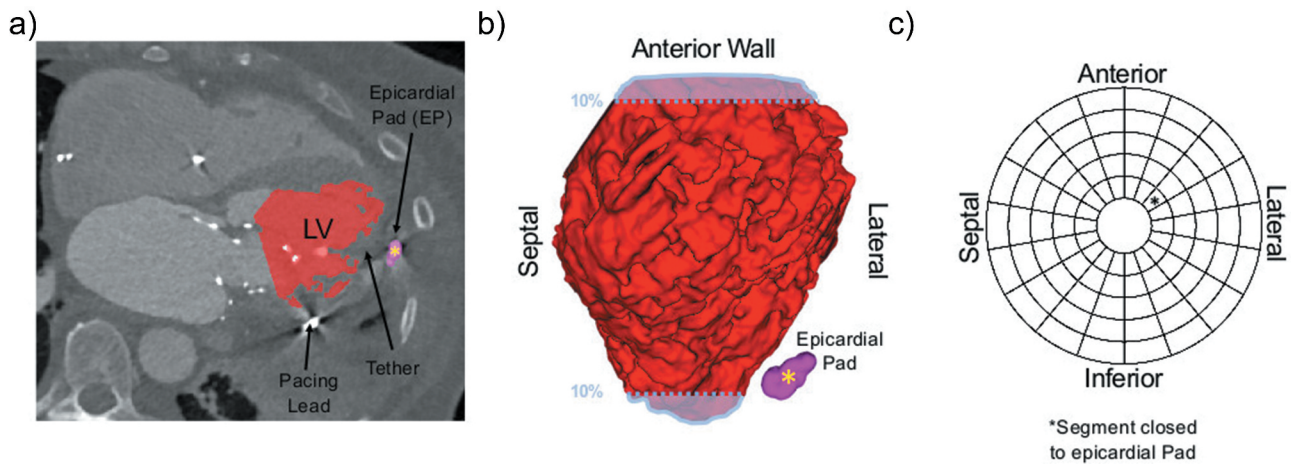
Figure 3. Identifying the location of the epicardial pad in the 4DCT data. (a) Axial view of segmented left ventricle (LV) and epicardial pad (EP), (b) 3D view of segmented LV and EP. Only when creating the bullseye plots, the top and bottom 10% of the ventricle are excluded due to higher registration errors in these regions, (c) Bullseye plot with 90 segments (18 circumferential x 5 longitudinal) marking the segment closest to the EP with an asterisk (*).

volumes and EF were significant across the 17 subjects, paired, two-sided Wilcoxon signed rank tests were performed with a significance level of $\alpha = 0.05$. Segmental changes in RS_{CT} between pre and post TMVI were also evaluated for significance using paired, two-sided Wilcoxon signed rank tests with significance level of $\alpha = 0.05$. These paired differences were evaluated in each subject for all 90 segments. In addition, analysis on the apical region (two inner rings of the bullseye) was performed to attempt to isolate the effect of the epicardial pad. These statistical tests were used instead of the student t-test for two reasons: 1) the small cohort size and 2) RS_{CT} was not normally distributed (evaluated using the Kolmogorov–Smirnov Test for Normality) in many of the subjects due to their highly abnormal LV function. Correlation coefficients and corresponding *p*-values were also computed between global and regional metrics of LV function derived from 4DCT.

Reproducibility of RS_{CT} in TMVI patients

Because of the variability in image quality, the highly abnormal LV geometries of Tendyne patients, and the wide dynamic range of peak RS_{CT} within each subject, we evaluated the reproducibility of our method for measuring high-resolution regional endocardial function in a subset of this group of patients. In order to quantify intra-observer variability, the first observer (Observer 1) who performed the RS_{CT} analysis on all 17 subjects re-segmented the ED and ES phases of the 5 patients with the largest decreases in EF post TMVI for both baseline and 1-month post TMVI 4DCT exams. Observer 1's second round of segmentations were performed at least 4 months after performing the original segmentation. These newly segmented timeframes were used to calculate RS_{CT} at ES and the 90 segment bullseye plots were compared with Observer 1's results from the first segmentation. Correlation and Bland-Altman plots were constructed to measure the variability.

For measurement of inter-observer variability, an Observer 2 was recruited to segment the same five patients at ED and ES for the pre and post TMVI exams. Observer 2's 90 segment bullseye plots were compared to Observer 1's two separate

analyses. Again, correlation and Bland-Altman plots were created to show the variability. To quantify a single average limit of agreement from the Bland-Altman between the two comparisons, the propagation of error rules was followed. The mean bias was calculated as the average of the two biases and the mean standard deviation computed as:

$$dT = \frac{\sqrt{(d_{12})^2 + (d_{22})^2}}{2} \tag{2}$$

where d_{12} is the standard deviation from Observer 1's first analysis and Observer 2 and d_{22} is the standard deviation from Observer 1's second analysis and Observer 2.

Results

Main findings

The baseline characteristics of the 17 subjects evaluated in this study are shown in Table 3. Comprehensive analysis of the changes in global and regional cardiac function post TMVI using 4DCT was performed on all 17 subjects and is illustrated in Figure 4 for an example subject. Due to the heterogeneous pattern of RS_{CT} at baseline, and the subsequent complex change in RS_{CT} post TMVI, we created this visual report for each patient in order to perform comparisons between subjects. In this report, we show the changes in 4DCT-derived global LV function through changes post TMVI in EDV, ESV, and EF (Figure 4a). High resolution maps of regional LV function at Baseline and 1-month post TMVI are shown side-by-side in 90 segment bullseye plots of peak RS_{CT} (Figure 4b); these maps show the original functional state of the LV, and the condition of the LV post TMVI. We enumerate the *changes* in RS_{CT} functional categories post TMVI in tabular form in Figure 4c; this summarizes the number of segments that increase contraction vs. decrease contraction post TMVI. These tabular results are also displayed in a bullseye plot to analyze the spatial patterns in these changes (Figure 4d). The "overall" changes in functional categories over the entire LV are captured in the histogram shown in Figure 4e which gives

Table 3. Baseline patient characteristics (N = 17).

Age, years	73.7 ± 8.6
BMI	26.3 ± 6.2
STS-PROM, %	6.1 ± 2.8
NYHA Functional Class	
II (%)	4 (23.5)
III (%)	12 (70.6)
IV (%)	1 (5.9)
Etiology of MR	
Primary (%)	1 (5.9)
Secondary (%)	16 (94.1)
Hospitalization for Heart Failure within 6 months (%)	3 (17.6)
History of Congestive Heart Failure (%)	13 (76.5)
Diabetes Mellitus (%)	5 (29.4)
Coronary Artery Disease (%)	11 (64.7)
Prior Myocardial Infarction (%)	7 (41.2)
Prior CABG (%)	5 (29.4)
Prior Percutaneous Coronary Intervention (%)	5 (29.4)
Pacemaker Implanted (%)	7 (41.2)
Prior Valve Intervention/Surgery (%)	0 (0)
Peripheral Artery Disease (%)	2 (11.8)
Current or Prior Smoker (%)	11 (64.7)
COPD (%)	10 (58.8)
Hypertension	13 (76.5)
GFR < 60, mL/min	10 (58.8)
Medications	
ACE Inhibitor or ARB (%)	10 (59.8)
Beta-receptor antagonist (%)	14 (82.4)
Vasodilator (%)	1 (5.9)
Diuretic (%)	14 (82.4)
Digoxin (%)	3 (17.6)
Anticoagulant (%)	9 (52.9)

the viewer an immediate appreciation of the total number of segments changing their functional status.

From this preliminary study, it was clear from the RS_{CT} difference maps (Figure 4b) that the mechanical response to TMVI was highly variable between subjects, and the patterns of the change in RS_{CT} (Figure 4d) were highly localized and heterogeneous over the LV. Figure 5 contains illustrative comparisons between subjects with similar relative decreases in EF but regionally different mechanical responses to TMVI and are discussed further below.

Example comparisons between subjects with similar changes in ejection fraction

In this section, by way of two comparisons, we show the variable nature of both the original myocardial function pattern and the very different local response to TMVI while generating the same response according to EF.

Comparison 1: Subjects 1 and 2 in Figure 5 had baseline EFs ~39% and showed the same decrease in this global parameter after TMVI. Yet, their baseline functional maps were very different ($p < 0.05$) and the changes in RS_{CT} post implantation were also very different as shown in Figure 5a. At baseline, subject 2 displayed global hypokinesia with some higher functioning tissue

located in the apex. After TMVI, RS_{CT} in the apex was greatly reduced. For subject 1, at baseline a larger portion of tissue outside the apex on the anterior and antero-lateral wall was functioning well (20% was normal/kinetic in this region compared to 5% for subject 2). After TMVI, the magnitude of RS_{CT} *increased* in the anterior and antero-lateral apical region despite placement of the epicardial pad in the apex. In both subjects there was reduced function observed outside of the apical region. While an expected reduction in RS_{CT} is seen in many subjects in the apical regions near the epicardial pad, this does *not* explain the total change in local function as shown in these subjects.

Comparison 2: Subjects 3 and 4 had high pre-TMVI EFs for this cohort (~58%) and had similar decreases in EF post-TMVI, which is consistent with elimination of the substantial regurgitant volume. At baseline, subject 3 had mostly normal or kinetic tissue while subject 4 had a small region of hypo-kinetic tissue on the infero-septal wall. Post TMVI, patient 4 lost some function in the local region near the EP while subject 3 lost much more normal or kinetic tissue at the apex and surrounding tissue, as is evident in Figure 5b. However, in subject 3 there was a small region of tissue on the basal-inferior wall that has increased RS_{CT} post-procedure, while there was no localized change in RS_{CT} in subject 4 outside the apex.
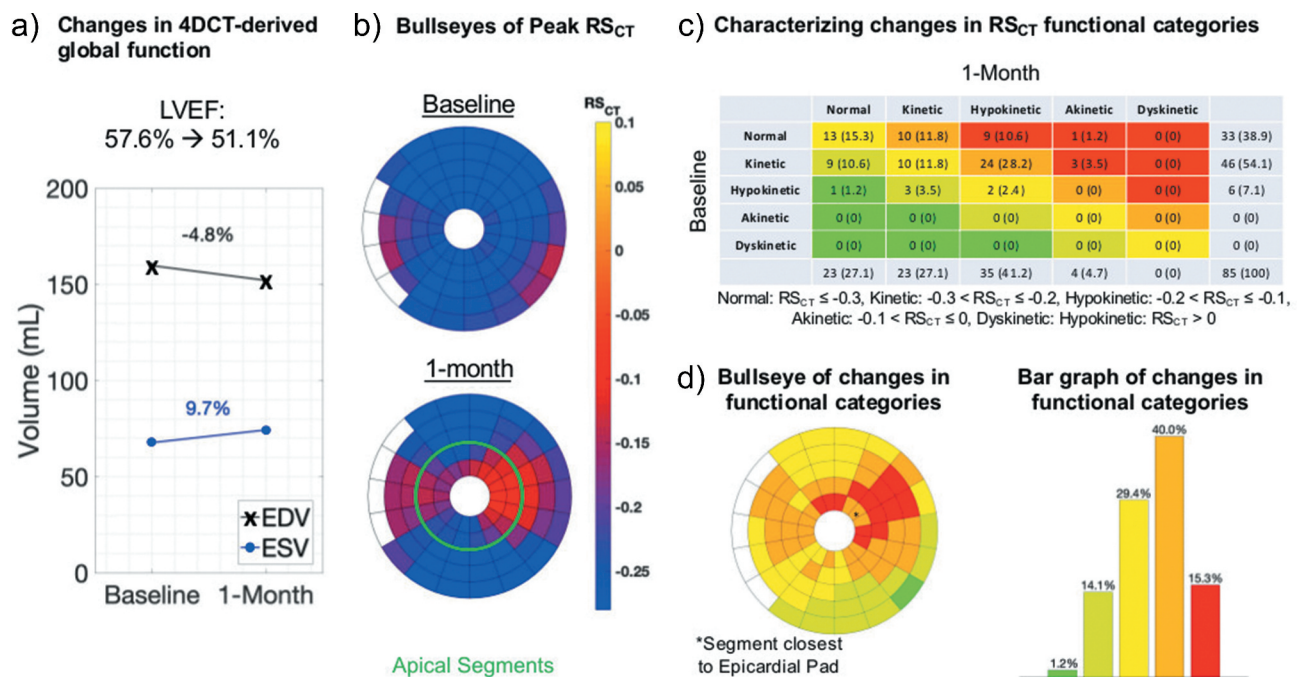
Figure 4. Comprehensive visual analysis of 4DCT-derived regional and global metrics of cardiac function for an example patient. (a) 4DCT-derived end-diastolic (ED) and end-systolic (ES) volumes were computed and used to calculate ejection fraction (EF) pre and post TMVI, (b) Bullseye plots of peak RS_{CT} at baseline and 1-month post TMVI. The apical segments were defined as the two inner rings of the bullseye, (c) Characterization of changes in regional function between baseline and 1-month: segments that did not change are shown in yellow, those that decreased by 1 category are orange, those that increased by 1 category are light green, and those that decreased or increased by 2+ categories are red or bright green, respectively, (d) Bullseye plot showing the spatial distribution of the changes categorized in panel C, and (e) Bar graph displaying the percentage of segments in a category from panel C.

Reproducibility of RS_{CT}

Both intra- and inter-observer variability were similar as shown in Figure 6a and 6b. Segmental end-systolic RS_{CT} values were highly correlated for all three comparisons and the bias was small. The 95% confidence limit on the Bland-Altman plots for intra-observer variability was ±0.061 and for inter-observer variability it was ±0.053 as an average for the two comparisons. In addition, Figure 6c shows for an example subject the 90 segment bullseye plots comparing Observer 1's first analysis, Observer 1's second analysis, and Observer 2's analysis. Despite small differences in RS_{CT}, the main features of these spatially heterogeneous regional shortening maps are extremely similar for all three analyses.

Observations of global LV metrics

In this small cohort of patients, there was a statistically significant change in ED volume post TMVI but no significant change in other global parameters such as ES volume ($p = 0.46$), or EF ($p = 0.10$). EF changed by less than 5% in six subjects. Three subjects had an increase in EF with two subjects increasing between 5% and 10% and one patient increasing more than 10%. Eight subjects had a decrease in EF with five subjects decreasing between 5% and 10% and three subjects decreasing more than 10%.

There was a wide diversity in the spatial patterns of regional function in both the pre and post TMVI hearts. Ten of the 17 subjects had 50% or more LV segments characterized as hypokinetic, akinetic, or dyskinetic ($RS_{CT} > -0.20$) at baseline. When analyzed in aggregate, the total number of segments classified as normal or kinetic tissue highly correlated with EF ($R = 0.94$, $p < 0.05$) as expected (Figure 7a). Also, a decrease in EF post TMVI correlated with the percentage of segments that decreased by 1 or more functional categories ($R = 0.78$, $p < 0.05$) (Figure 7b). Eight subjects showed a significant ($p < 0.05$) positive shift in the distribution of RS_{CT} evaluated over all 90 segments using the two-sided, paired segmental Wilcoxon Signed rank test. This net positive shift of the classification of the segments corresponds to an overall decrease in LV function. Three subjects showed a significant ($p < 0.05$) negative shift in the distribution of RS_{CT} over all 90 segments. Lastly, six subjects had a significant change in RS_{CT} ($p < 0.05$) when looking only at the apical region (inner 18 segments of the bullseye). In some subjects, there was a clear reduction in the magnitude, or absolute value, of RS_{CT} in the region of the EP, whereas in other subjects there was little or no change. Overall, a reduction of greater than 5% of normal or kinetic tissue in the LV and in the apex lead to a decrease in EF post TMVI. These are preliminary observations, however, and the small number of patients preclude analysis of trends in these data.

Discussion

Main findings

In this paper, we introduce a reproducible, high-resolution method (90 LV segments) for evaluating regional changes in LV endocardial shortening before and 1-month after TMVI using 4DCT (RS_{CT}). These measurement of RS_{CT}, integrated with traditional clinical parameters and biomarkers, provide
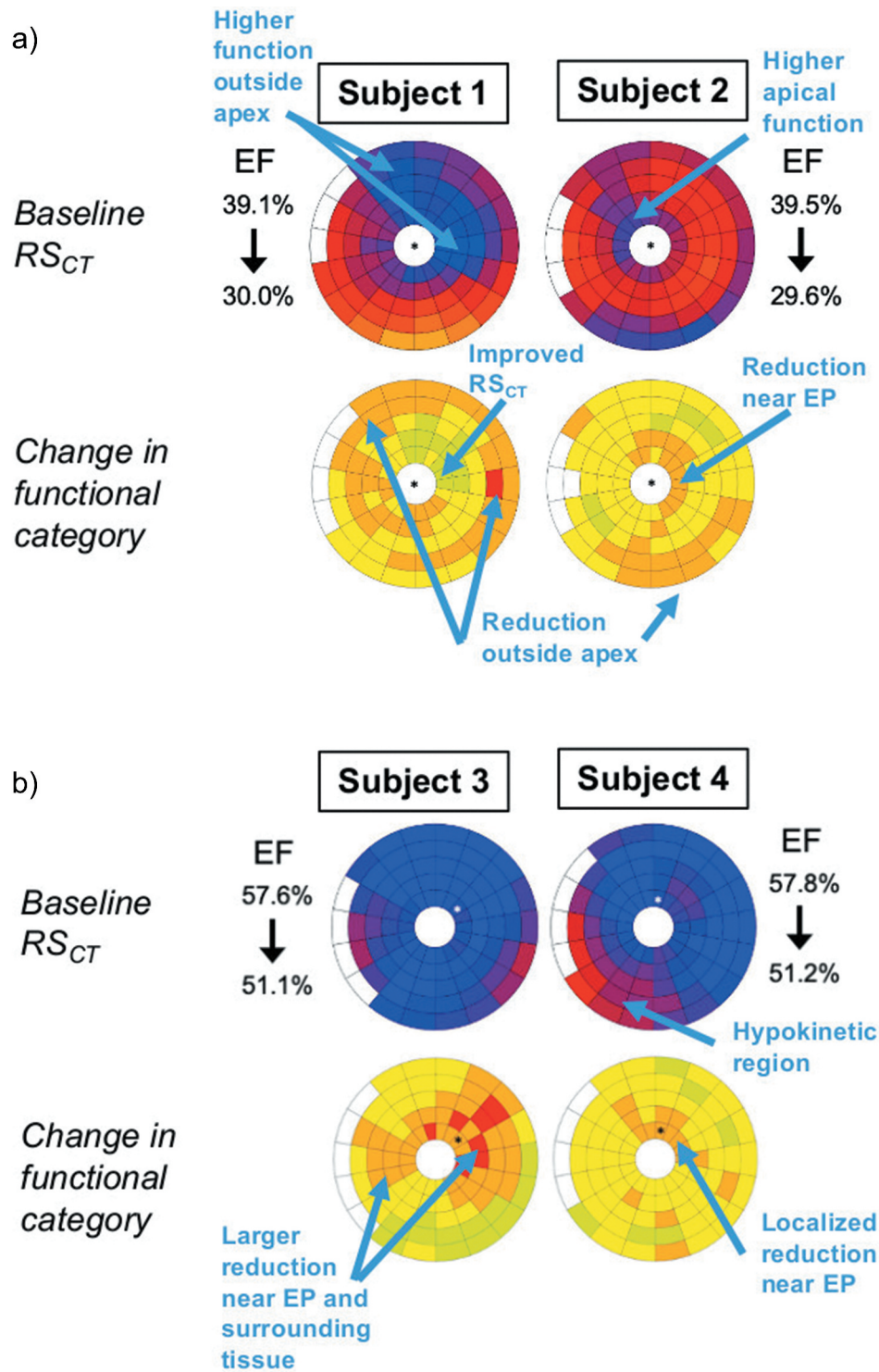
Figure 5. Two comparisons of baseline RS_{CT} patterns and changes in RS_{CT} 1-month after TMVI in subjects with similar relative changes in ejection fraction. Example subjects are highlighted for comparison of baseline RS_{CT} patterns and changes in RS_{CT} 1-month after TMVI: (a) subjects 1 and 2 showing decreased ejection fraction (EF) after TMVI and (b) subjects 3 and 4 showing decrease in EF but relatively higher baseline EF. Regions of interest are labeled for each of these comparisons. *Epicardial Pad (EP).

a more comprehensive analysis of the state of the heart and spatially detailed response to TMVI.[8] The majority of TMVI patients will undergo a contrast-enhanced 4DCT scan prior to the procedure to obtain annular measurements for device sizing.[3,4,19] It is recommended that for these measurements, images should be acquired across the entire cardiac cycle given the dynamic changes in the anatomical configuration of the LV, LVOT, and mitral valve apparatus[4,24]; therefore, our proposed analysis of regional LV function from the 4DCT images can be performed without extra radiation. In fact, large retrospective studies can be performed on existing data such as the Expanded Clinical Study of the Tendyne Mitral Valve System (NCT02321514) and Tendyne SUMMIT Clinical Trial (NCT03433274).
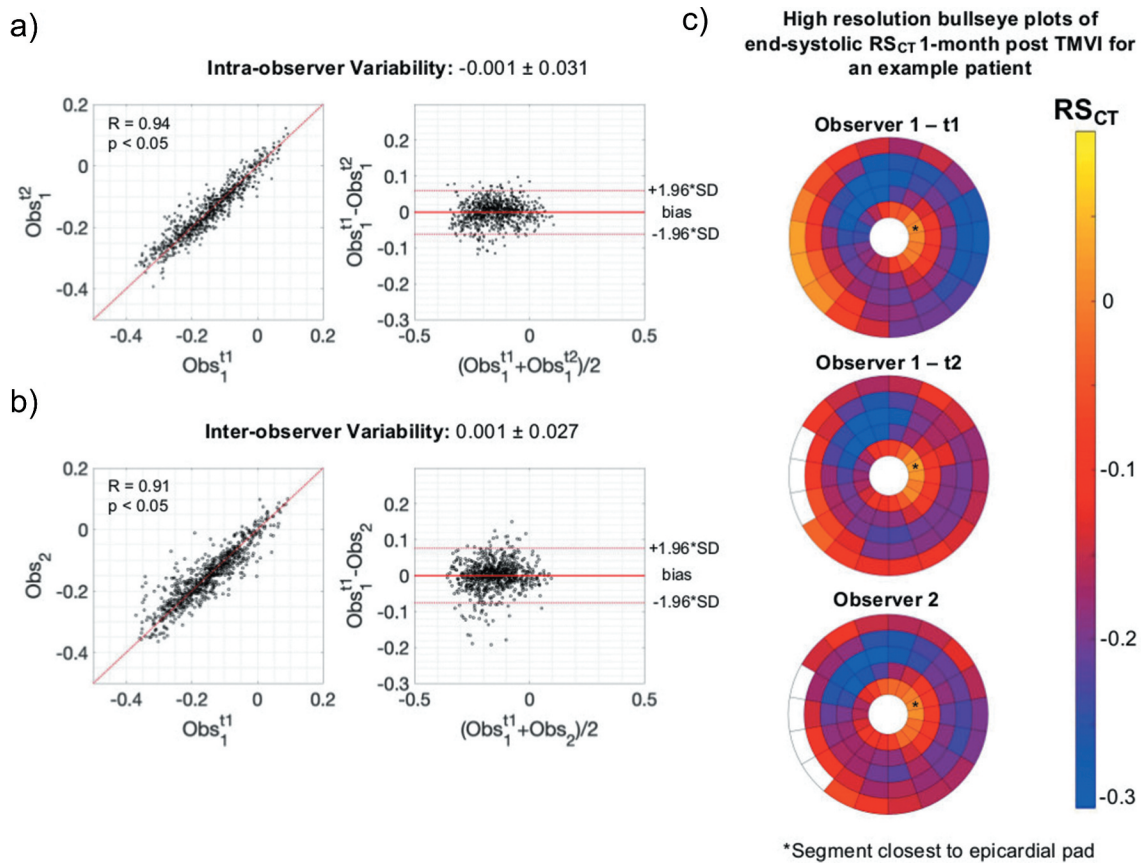
Figure 6. Reproducibility of RS_{CT} in TMVI patients. Correlation and Bland-Altman Plots comparing (a) Observer 1's first (t2) and second analysis (t2), (b) Observer 1's first analysis (t2) with Observer 2's analysis for a subset of 5 subjects for both baseline and 1-month 4DCT exams. (c) High resolution bullseye plots of end-systolic RS_{CT} for an example patient 1-month post TMVI for all 3 independent analyses.

Despite their highly abnormal LV function and geometries, we were able to obtain high resolution estimates of RS_{CT} in all 17 subjects. The results of the reproducibility study performed on these subjects show that the 95% confidence intervals are about 12% and 10% of the total dynamic range of RS_{CT} values observed in this patient population (about -0.39 to $+0.12$), respectively. Therefore, the measurement of RS_{CT} is a highly precise estimate of local LV function. It is evident from this initial proof-of-concept study that RS_{CT} patterns and the local changes in the mechanical response post implantation were extremely heterogeneous across all subjects assessed. While the majority (N = 14) of subjects saw a less than 10% change in EF after the procedure, 11/17 (64.7%,) had a significant spatially heterogeneous changes in RS_{CT} across the entire LV, while the remaining 6/17 (41.2%) had significant changes just in the apical region. This result indicates that the functional states of these TMVI patients cannot be fully characterized with global parameters such as ED volume, ES volume, and EF. In addition, for patients with severe MR, EF may not capture the full picture of LV function because a significant proportion of the stroke volume flows retrograde into the left atrium and does not contribute to systemic perfusion.[8]

Lastly, the resulting change in LV function after TMVI near the location of the epicardial pad had not yet been characterized. In this study, we were able to evaluate changes in RS_{CT} with high spatial resolution in the local region near the epicardial pad. We observed a highly variable effect of the epicardial pad on the local myocardial function in this small patient cohort; function can either decrease markedly, or even increase. The ability to resolve this kind of detail may prove useful in optimizing implantation procedures with larger patient datasets.

Limitations

The primary limitation of this preliminary study is the small number of patients analyzed (17 total) which precludes correlation of these results with clinical outcomes. However, the results demonstrate that regional shortening from CT can measure both the baseline state of the endocardium, and changes in regional cardiac function with high spatial resolution and high precision without making *a priori* assumptions about LV geometry on a wide variety of scanners. The 4DCT exams for the 17 total patients analyzed were acquired on 4 different scanner platforms and were obtained retrospectively for this study. As shown in Table 1, if images of sufficient quality were obtained, the analysis could be performed. With recent advances in CT scanners, including wide-detector technology, dual source x-ray, and high pitch acquisition platforms, ED and ES phases can be acquired in a single heartbeat
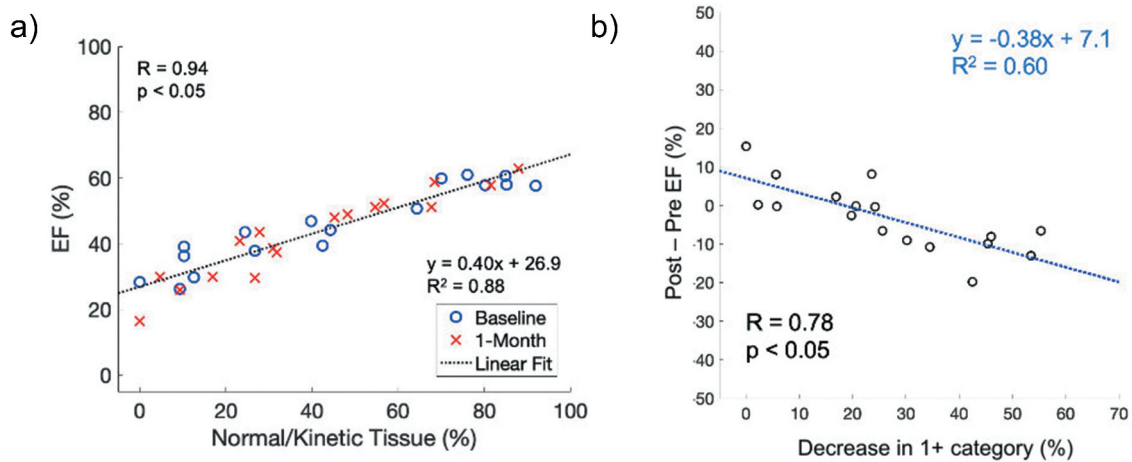
Figure 7. Amount of normal and kinetic tissue in the left ventricle and a decrease in mechanical function correlates with ejection fraction. (a) Ejection fraction (EF) is correlated with the percentage of normal/kinetic tissue in the left ventricle at baseline and 1-month after TMVI. Normal and kinetic tissue was defined any segment with $RS_{CT} \leq -0.2$. (b) A change in EF is correlated with the percentage of tissue with decreases in 1 or more regional shortening categories.

and at very low x-ray dose.[5,13] Poor image quality from step artifacts can be avoided with single-beat CT technology.

Future work

Equipped with detailed maps of regional function, combined with clinical and procedure-related parameters, retrospective analysis of a larger patient cohort could provide an integrative approach for assessment of cardiac structure and function beyond EF and chamber volumes.[8] Recently, a study by Fukui *et al.* showed that closer proximity of the EP to the true apex was predictive of favorable LVEDV reverse remodeling.[25] Combining the results of this global functional analysis with our proposed regional evaluation of cardiac function could lead to a more precise understanding of the effect of MR and TMVI on regional LV function and remodeling and help determine which patients will benefit from valve replacement. We created a comprehensive LV function characterization report as shown in Figure 4 which can be used for this analysis. Lastly, the methods developed herein can also be used to optimize other structural heart therapies in addition to TMVI.

Conclusions

We introduce a method for measuring detailed 3D regional LV function in patients before and 1-month after TMVI using 4DCT. We demonstrate that is it feasible to reproducibly measure regional shortening (RS_{CT}) in these subjects who have highly abnormal regional LV function and highly abnormal geometry from ED and ES phases with high precision. Significant regional changes in RS_{CT} were observed following TMVI in all subjects, with high variability between the subjects evaluated. The regionally heterogeneous LV functional state of TMVI patients cannot be fully described by changes, or lack thereof, in global parameters such as ED and ES volumes, nor EF. Future studies will aim to evaluate the clinical usefulness of the highly reproducible 4DCT-based method introduced in this proof-of-concept study. In general, we hope this method can be

used to increase our understanding of the effects of TMVI and other transcatheter therapies on regional cardiac function.

ORCID

Gabrielle M. Colvert http://orcid.org/0000-0001-5102-8650

Disclosure statement

JG: Employed full time at Abbott Laboratories
FJC: Receives research funding from Bayer Healthcare AG.
PB and JL: Provides institutional core lab services to Abbott, Edwards, Medtronic, PI Cardia, Boston Scientific and is a consultant to Circle CVI, MVRX, Edwards, and Abbott.
JL: Received research grants from Edwards and GE Healthcare
ERM: Holds founder shares in Clearpoint Neuro Inc. and receives research funding from GE Healthcare, Abbott Medical, and Pacesetter Inc.

References

1. Blanke P, Weir-mccall JR, Achenbach S, et al. Computed tomography imaging in the context of Transcatheter Aortic Valve Implantation (TAVI)/Transcatheter Aortic Valve Replacement (TAVR). *JACC Cardiovasc Imaging.* 2019;12(1):1–24. doi:10.1016/j.jcmg.2018.12.003.
2. Bouma BJ, Mulder BJM. Changing landscape of congenital heart disease. *Circ Res.* 2017;120(6):908–922. doi:10.1161/CIRCRESAHA.116.309302.
3. Muller DWM, Farivar RS, Jansz P, et al. Transcatheter mitral valve replacement for patients with symptomatic mitral

regurgitation: a global feasibility trial. *J Am Coll Cardiol.* 2017;69 (4):381–391. doi:10.1016/j.jacc.2016.10.068.

4. Blanke P, Naoum C, Webb J, et al. Multimodality imaging in the context of transcatheter mitral valve replacement establishing consensus among modalities and disciplines. *JACC Cardiovasc Imaging.* 2015;8(10):1191–1208. doi:10.1016/j.jcmg.2015.08.004.

5. Nicol ED, Norgaard BL, Blanke P, et al. The future of cardiovascular computed tomography: advanced analytics and clinical insights. *JACC Cardiovasc Imaging.* 2019;12(6):1058–1072. doi:10.1016/j.jcmg.2018.11.037.

6. Carminati M, Agnifili M, Arcidiacono C, et al. Role of imaging in interventions on structural heart disease. *Expert Rev Cardiovasc Ther.* 2013;11(12):1659–1676. doi:10.1586/14779072.2013.854166.

7. Nishimura RA, Otto CM, Bonow RO, et al. 2017 AHA/ACC Focused Update of the 2014 AHA/ACC guideline for the management of patients with valvular heart disease: a report of the American College of Cardiology/American Heart Association Task Force on Clinical Practice Guidelines. *Circulation.* 2017;135 (25):e1159–e1195. doi:10.1161/CIR.0000000000000503.

8. Cikes M, Solomon SD. Beyond ejection fraction: an integrative approach for assessment of cardiac structure and function in heart failure. *Eur Heart J.* 2016;37(21):1642–1650. doi:10.1093/eurheartj/ehv510.

9. Smiseth OA, Torp H, Opdahl A, Haugaa KH, Urheim S. Myocardial strain imaging: how useful is it in clinical decision making? *Eur Heart J.* 2016;37(15):1196–1207b. doi:10.1093/eurheartj/ehv529.

10. Cardinale D, Colombo A, Bacchiani G, et al. Early detection of anthracycline cardiotoxicity and improvement with heart failure therapy. *Circulation.* 2015;131(22):1981–1988. doi:10.1161/CIRCULATIONAHA.114.013777.

11. Kalam K, Otahal P, Marwick TH. Prognostic implications of global LV dysfunction: a systematic review and meta-analysis of global longitudinal strain and ejection fraction. *Heart.* 2014;100 (21):1673–1680. doi:10.1136/heartjnl-2014-305538.

12. Kamperidis V, Marsan NA, Delgado V, Bax JJ. Left ventricular systolic function assessment in secondary mitral regurgitation: left ventricular ejection fraction vs. speckle tracking global longitudinal strain. *Eur Heart J.* 2016;37(10):811–816. doi:10.1093/eurheartj/ehv680.

13. Chen MY, Arai AE. Submillisievert median radiation dose for coronary angiography with a second-generation. *Radiology.* 2013;267(1):76–85. doi:10.1148/radiol.13122621/-/DC1.

14. Pourmorteza A, Chen MY, van der Pals J, Arai AE, McVeigh ER. Correlation of CT-based regional cardiac function (SQUEEZ) with myocardial strain calculated from tagged MRI: an experimental study. *Int J Cardiovasc Imaging.* 2016;32 (5):817–823. doi:10.1007/s10554-015-0831-7.

15. Sorajja P, Moat N, Badhwar V, et al. Initial feasibility study of a new transcatheter mitral prosthesis: the first 100 patients. *J Am Coll Cardiol.* 2019;73(11):1250–1260. doi:10.1016/j.jacc.2018.12.066.

16. Yushkevich PA, Piven J, Hazlett HC, et al. User-guided 3D active contour segmentation of anatomical structures: significantly improved efficiency and reliability. *Neuroimage.* 2006;31 (3):1116–1128. doi:10.1016/j.neuroimage.2006.01.015.

17. Otsu N. A threshold selection method from gray-level histograms. *IEEE Trans Syst Man Cybern.* 1979;9(1):62–66. doi:10.1109/tsmc.1979.4310076.

18. Colvert G, Manohar A, Colvert B, Schluchter A, Contijoch F, McVeigh ER. Novel measurement of LV twist using 4DCT: quantifying accuracy as a function of image noise. *Med Imaging 2019 Biomed Appl Mol Struct Funct Imaging.* 2019;(March):54. doi:10.1117/12.2512532.

19. Blanke P, Dvir D, Cheung A, et al. A simplified D-shaped model of the mitral annulus to facilitate CT-based sizing before transcatheter mitral valve implantation. *J Cardiovasc Comput Tomogr.* 2014;8(6):459–467. doi:10.1016/j.jcct.2014.09.009.

20. Ortuño-Fisac JE, Vegas-Sánchez-Ferrero G, Gómez-Valverde JJ, et al. Automatic estimation of aortic and mitral valve displacements in dynamic CTA with 4D graph-cuts. *Med Image Anal.* 2020;65:101748. doi:10.1016/j.media.2020.101748.

21. Pourmorteza A, Schuleri KH, Herzka DA, Lardo AC, McVeigh ER, New A. Method for cardiac computed tomography regional function assessment: SQUEEZ. *Circ Cardiovasc Imaging.* 2012;5:243–250. doi:10.1161/CIRCIMAGING.111.970061.

22. McVeigh ER, Pourmorteza A, Guttman M, et al. Regional myocardial strain measurements from 4DCT in patients with normal LV function. *J Cardiovasc Comput Tomogr.* 2018;12(5):372–378. doi:10.1016/j.jcct.2018.05.002.

23. Pourmorteza A, Keller N, Chen R, et al. Precision of regional wall motion estimates from ultra-low-dose cardiac CT using SQUEEZ. *Int J Cardiovasc Imaging.* 2018;34(8):1277–1286. doi:10.1007/s10554-018-1332-2.

24. Bax JJ, Debonnaire P, Lancellotti P, et al. Transcatheter interventions for mitral regurgitation: multimodality imaging for patient selection and procedural guidance. *JACC Cardiovasc Imaging.* 2019;12(10):2029–2048. doi:10.1016/j.jcmg.2019.03.036.

25. Fukui M, Sorajja P, Gössl M, et al. Left ventricular remodeling after transcatheter mitral valve replacement with tendyne: new insights from computed tomography. *JACC Cardiovasc Interv.* 2020;13(17):2038–2048. doi:10.1016/j.jcin.2020.06.009.